journal

J. Am. Ceram. Soc., 99 [5] 1594–1600 (2016)
DOI: 10.1111/jace.14186
© 2016 The American Ceramic Society

Polyamorphism in Aluminum Nitride: A First Principles Molecular Dynamics Study

Murat Durandurdu†

Department of Materials Science & Nanotechnology Engineering, Abdullah Gül University, Kayseri 38080, Turkey

The high-pressure behavior of amorphous aluminum nitride is investigated for the first time by means of *ab initio* molecular dynamics simulations. It is found to undergo two successive first-order phase transformations with the application of pressure. The first one is a *polyamorphic* phase transition in which the low-density amorphous phase transforms into a high-density amorphous phase having an average coordination number of about 4.6. The high-density amorphous structure transforms back to a low-coordinated amorphous network upon pressure release but its density is higher than that of the original low-density amorphous phase. The second phase change is the crystallization of the high-density amorphous state into a rocksalt structure. A careful analysis suggests that the hexagonal-like nanoclusters presented in amorphous aluminum nitride prevent the formation of a very dense amorphous phase (about sixfold coordinated) during the first phase transition and they act as a nucleation center for the crystallization process.

I. Introduction

Aluminum Nitride (AlN), an important ceramic of considerable current interest, has both crystalline and amorphous forms.[1–6] Crystalline AlN has been studied extensively for last few decades and its remarkable properties, and possible technological applications have been discussed in details.[7–12] It has a high melting temperature and a thermal stability, which make AlN a suitable material for refractory applications[13] and high-temperature electronics, for example, ultra-high-temperature piezoelectric sensors.[14] It is also used in the microelectronic industry such as electronic packaging, heat sink, etc.[15,16] due to its high thermal conductivity.

For the case of amorphous AlN (*a*-AlN), regrettably its properties and its potential high-tech applications are still far from our understanding because of limited investigations on it. The doped *a*-AlN with rare earth elements appears to have some practical applications for optical, photonic, and electronic devices.[17–22]

The ground state of AlN is the hexagonal wurtzite (WZ) structure having space group $P6_3mc$[1] but the formation of a metastable zinc blende (ZB) type of AlN within $F\bar{4}3m$ symmetry was also reported in an experiment under some specific conditions.[2] For *a*-AlN, its microstructure has not been discussed in any experiment, to our knowledge, but theoretical studies based on first principles molecular dynamic (MD) techniques reported that the local structural arrangement of *a*-AlN appears to be partially different from the crystalline phases because the computer generated amorphous models present the edge-sharing units (four membered rings)[23,24] and three-dimensional hexagonal-like nanoclusters embedded in the amorphous matrix,[24] neither of which exists in the crystalline states. The presence of these unusual clusters might lead to new research on *a*-AlN and possible its applications in nanotechnology.

Because of its high technological relevance, the behavior of the WZ-AlN under extreme conditions is also of interest.[25–38] The pressure-induced first-order phase transformation from the WZ structure to the rocksalt (RS) structure ($Fm\bar{3}m$) was reported in several experiments.[25–27] This phase transition exhibited a quite large hysteresis and upon pressure release, the RS structure did not transform back to the ground state[25] and instead it persisted at atmospheric pressure. The WZ-to-RS phase transformation was analyzed using the quantum mechanical calculations as well and the phase transition was predicted to take place at about 8.3–16.0 GPa,[29–38] fairly agreeing with the experimental transition pressures of 14.0–22.0 GPa.[25–27] Moreover, the transformation mechanism from the WZ phase into the RS crystal was investigated by means of a constant pressure *ab initio* MD technique and two five-fold-coordinated intermediate phases within $P6_3/mmc$ and *Cmcm* symmetries were proposed for this reconstructive phase transformation.[39]

For the case of *a*-AlN, to our knowledge, no high-pressure investigation has been reported in the literature so far but based on the previous experimental and computational analyses on insulating or semiconducting amorphous systems, two possible scenarios at room temperature can be considered for *a*-AlN. It can either transform into a crystalline phase or transform into a high-density amorphous (HDA) phase having different bonding environments, a phenomenon commonly observed in tetrahedrally coordinated disordered materials.[40–59] The phase transformation into a HDA phase under pressure is of not only scientific interest but also technological interest because it implies a way to produce new amorphous materials with the same composition but with different optical, mechanical, or electrical properties.[48,51]

In this work, the response of *a*-AlN to high pressure is, for the first time, investigated using an *ab initio* constant pressure MD method that was successfully applied to probe the WZ-to-RS phase transition of AlN[39] and to model *a*-AlN.[24] Two successive first-order phase transitions in *a*-AlN are observed through the MD simulations. AlN undergoes a *polyamorphic* phase change (first-order amorphous-to-amorphous phase transition) before it crystallizes into a RS structure with the application of pressure. The HDA phase is semiconducting and has a band gap energy larger than that of the LDA phase.

II. Methodology

We performed MD simulations using a well tested *ab initio* code, SIESTA.[60] The method is based on the density functional theory (DFT) and uses a localized linear combination of atomic orbitals as basis sets. The Troullier and Martins scheme was applied to construct norm-conserving pseudopotentials.[61] The exchange-correlation energy was estimated by

W.-Y. Ching—contributing editor

Manuscript No. 37529. Received September 19, 2015; approved January 25, 2016.
†Author to whom correspondence should be addressed. e-mail: murat.durandurdu@agu.edu.tr

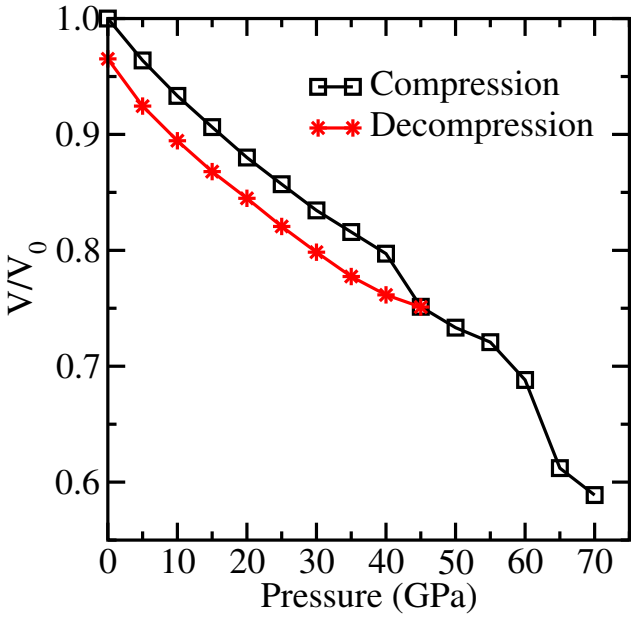

Fig. 1. Equation of state of *a*-AlN upon compression and decompression.

means of the generalized gradient approximation that implemented the Becke gradient exchange functional[62] and the Lee, Yang, Parr correlation functional.[63] The double zeta plus polarized orbitals were employed. A uniform mesh with a cutoff of 120 Ryd was used to represent the electron density, the local part of the pseudopotentials, and the Hartree and the exchange-correlation potential. An *a*-AlN model was generated using the same simulation technique from the liquid state (see Ref. [24] for more information) consisting of 216 atoms with periodic boundary conditions. We used Γ point sampling for the Brillouin zone integration. External pressure was controlled by the Parrinello–Rahman method[64] and increased progressively by an increment of 5 GPa. A period of 6000 MD steps was found to be reasonable to have the equilibrium volume at each applied pressure. Yet additional 5000 MD steps were run at and before the phase transformations to ensure that the system reached to the true equilibrium state. The time step of each MD simulation was one femtosecond. During the MD simulations, the power quenching technique was adopted, in which the velocity components for atoms or simulation box were set to zero when the velocities and forces had opposite signs. To visualize the structures the VESTA[65] program was used. As pointed out before, the Parrinello–Rahman method implemented in the SIESTA code was very successful in reproducing experimentally observed phase transition in AlN and predicting intermediate states for the WZ-to-RS phase transition.[39]

III. Results

The equation of state of *a*-AlN under pressure is illustrated in Fig. 1. The volume exhibits a sharp modification at 45 and 65 GPa. The volume dropped at 45 and 65 GPa is about 6% and 11%, respectively. Based on an abrupt volume dropped and a noticeable increase in the average coordination number (see below) at these pressures, the phase transitions in *a*-AlN are thermodynamically classified as a first-order phase transformation.

In order to have an atomic level description of the structure at these critical pressures and to understand the pressure-induced local structural rearrangements, the partial pair distribution functions (PPDFs), given in Fig. 2, are considered primarily. As understood from the figure, owing to the first phase transition at 45 GPa, the structure still remains amorphous because the PPDFs do not represent the

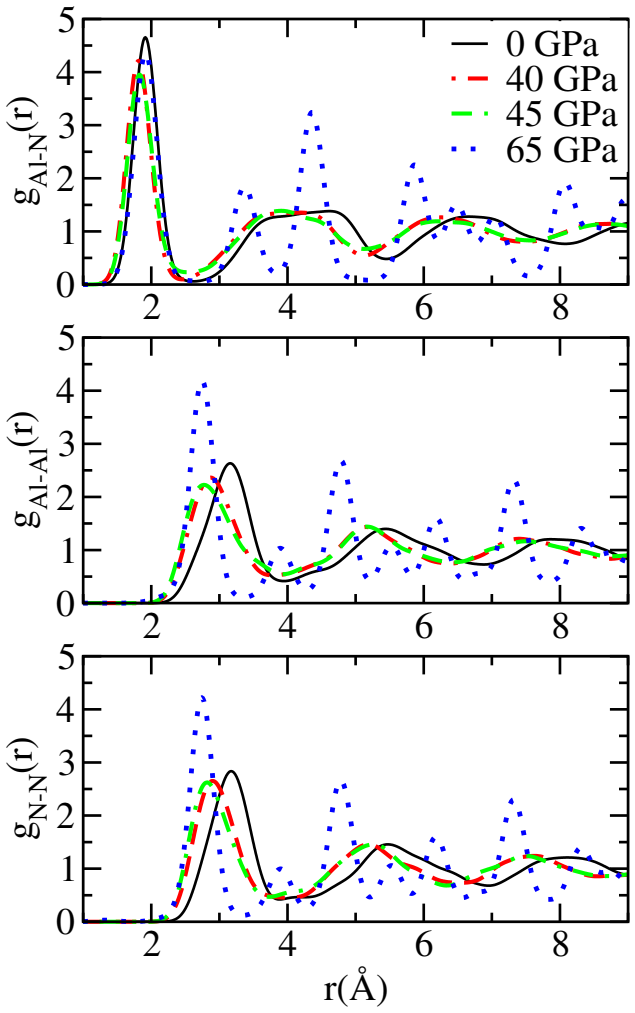

Fig. 2. Partial pair distribution functions (PPDFs) at selected pressures.

long-range correlations. This observation can be interpreted as the occurrence of a first-order amorphous-to-amorphous phase transformation (polyamorphic) in *a*-AlN. On the other hand, as for the second phase transformation at 65 GPa, the pronounced peaks at the long-range correlations obviously demonstrate a pressure-induced ordering in the model. The crystallization is visibly reflected in the PPDFs but the polyamorphic phase transition is not since there are no apparent drastic changes observed in the general shape of the PPDFs except that the position of the first peak of the Al-N correlation shifts slightly to a higher distance at 45 GPa as shown in Fig. 3. This shift is associated with a noticeable increase in the coordination number (CN). The HDA phase at 45 GPa and the crystalline phase at 65 GPa are illustrated in Fig. 4. *a*-AlN crystallizes into a RS phase having some structural defects.

In a contrast to the PPDFs, bond angle distribution functions (BADFs) shown in Fig. 5 present a dramatic modification during both phase transformations. The main peak around 109° and subpeak near 90° at zero pressure are due to tetrahedral and edge-sharing configurations, respectively. The angles around 120° are principally due to hexagons (see Ref. [24]). It should be mentioned here that the BADFs do not exhibit significant amendments except a small variation in the intensity of the main peak/subpeak and the appearance of very feeble peaks beyond 150° and below 70° until the first phase transformation takes place at 45 GPa. This means that the amorphous network undergoes insignificant structural rearrangements up to 45 GPa. Owing to the first phase transformation, the subpeak around 90° is considerably pronounced

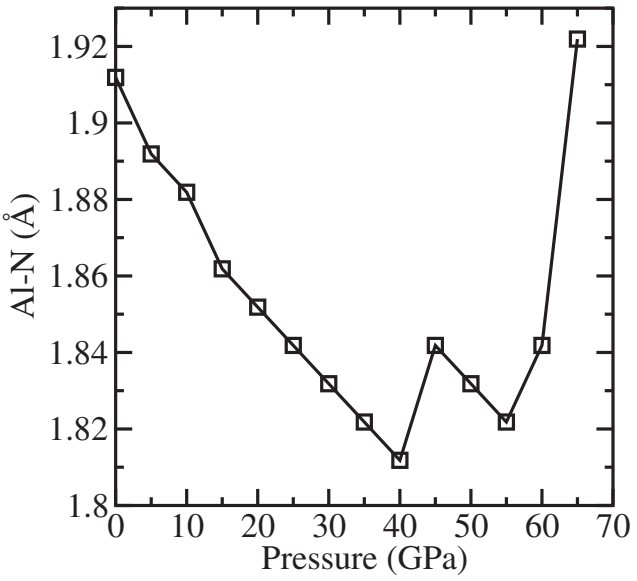

Fig. 3. The first peak position of the Al-N separation as a function of pressure.

and becomes the main peak in the both distributions, whereas the tetragonal angle peak around 109° is severely suppressed. Note that the suppression of this peak does not mean that the tetrahedral configurations are completely disappeared in the structure. As will be discussed below, they still exist in the model but the local structural units (fourfold rings) producing angles around 90° are dominated. The existence of a weak subpeak around 109° in the Al-N-Al distribution after the first phase change denotes that N-atoms have tendency to reserve more tetrahedral configurations than Al-atoms. Additionally, the presence of a subpeak around 120° suggests that hexagons still persist in the HDA phase of AlN.

Since pressure-induced amorphous-to-amorphous phase transitions are commonly identified by the coordination modification in nonmetallic systems, we next investigate the CN as a function of pressure and exhibit our data in Fig. 6. As realized from the figure, the CN increases marginally up to 45 GPa, at which point it suddenly jumps to a value of 4.6. Further increase in pressure results into a gradual increase in the CN initially and a second jump to 5.97 at 65 GPa. An analysis of the coordination distribution suggests that in the HDA state, about 51% of atoms are fivefold or higher coordinated and the rest are fourfold coordinated. Consequently, this phase transformation can be classified as a partial phase transformation. At 65 GPa, most atoms are sixfold coordinated as anticipated. Unexpectedly at each applied pressure, the partial average CN of Al and N is found to exactly overlap with the total average CN of the system although their coordination distribution is slightly different. For example at 45 GPa, fourfold, fivefold, and sixfold coordination are about 49%, 44%, and 7%, respectively for Al while they are near 50%, 42%, and 8% for N-atoms.

In order to find the structural relation between the HDA and high-pressure crystalline phases of AlN, a detailed description of the short-range order of the HDA state must be provided. Such a description further allows us to better understand the pressure-induced phase transitions. A comprehensive study of the local structure of the HDA phase suggests that the fourfold- and sixfold-coordinated atoms are tetragons and octahedrons, respectively, whereas the fivefold-coordinated configurations are incomplete octahedrons with missing one atom. They have a central atom surrounded by five atoms having a pyramid shape (see Fig. 7). The central atom and its four neighbors are unevenly on the base of the pyramid and its fifth neighbor is on the plane passing through the top vertex and perpendicular to the base of

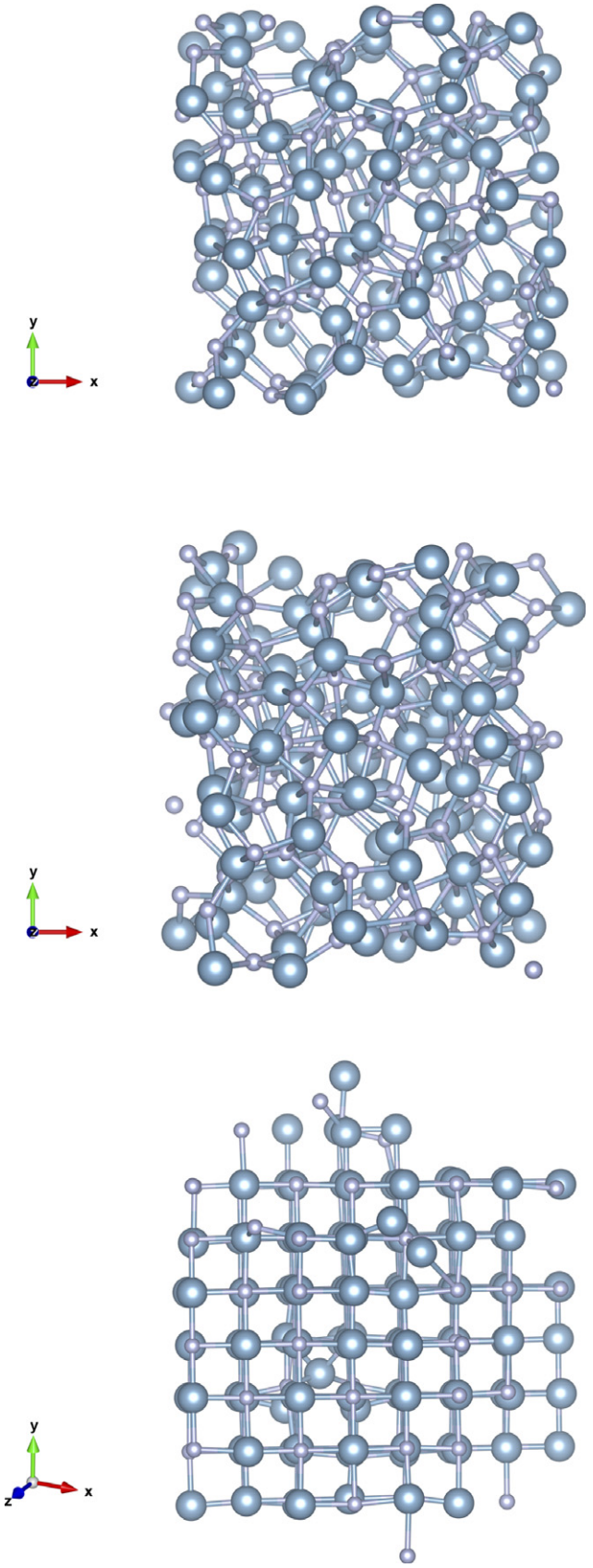

Fig. 4. Low-density amorphous (LDA) phase at zero pressure (upper panel). High-density amorphous phase (HDA) formed at 45 GPa (middle panel). RS phase formed at 65 GPa (lower panel).

the pyramid. Here, one might ask whether the formation of fivefold-coordinated clusters at high pressure is physical in *a*-AlN since the WZ-AlN transforms directly to a

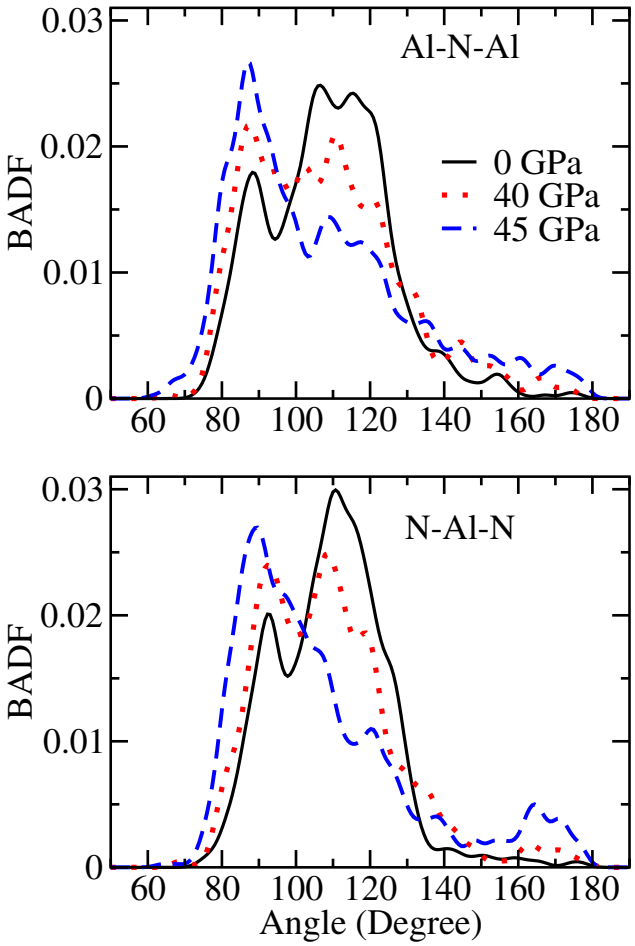

Fig. 5. The bond angle distribution functions (BADFs) at selected pressures.

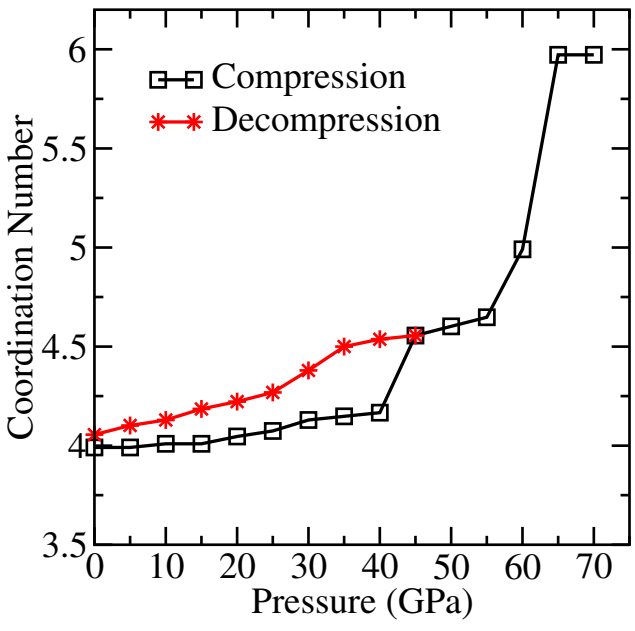

Fig. 6. Coordination number as a function of pressure.

sixfold-coordinated RS structure with the application of pressure. The answer is yes. Indeed the fivefold-coordinated two intermediate phases were proposed for the pressure-induced the WZ-to-RS phase transition.[39] The fivefold-coordinated clusters observed in *a*-AlN are surprisingly similar to ones formed in these intermediate phases (see Fig. 7). It should be

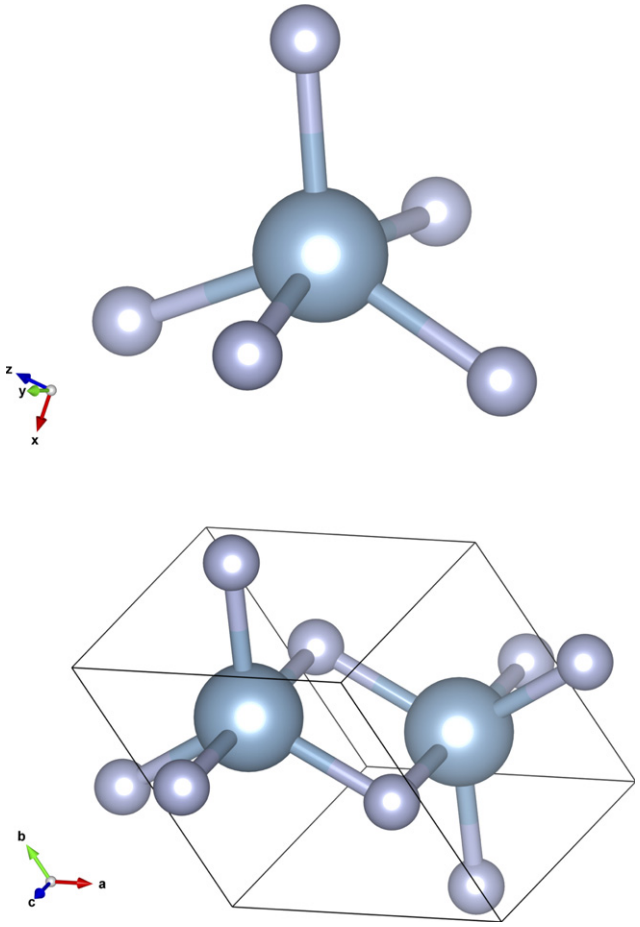

Fig. 7. Fivefold-coordinated cluster formed in *a*-AlN (upper panel). Intermediate *P*63/*mmc* phase formed during the WZ-to-RS phase transformation (lower panel).

pointed out here that the completely fivefold-coordinated structure is unstable in crystalline AlN.[39] An entirely fivefold-coordinated *a*-AlN is probably not stable too and hence a partial phase transformation occurs in *a*-AlN under pressure. Based on these findings, we can firmly state that the HDA phase carries the signature of the LDA phase (tetrahedral), the fivefold-coordinated intermediate phase(s) proposed for the WZ-to-RS phase transformation and little RS crystal. Consequently, the HDA phase of AlN might be characterized as *an amorphous intermediate phase* between the LDA phase and the RS crystal.

Upon pressure release, as shown in Fig. 1, the volume exhibits a hysteresis and the original volume is not recovered. On the other hand, as understood from Fig. 6, the CN decreases gradually upon decompression and reaches a value of about 4 at zero pressure. This means that a densified low-coordinated amorphous network is recovered on decompression. A careful consideration using both PPDFs and BADFs reveals that the short-range of the uncovered *a*-AlN upon pressure release is not noticeably different from that of the original model. On the basis of these results, we openly conclude that the amorphous-to-amorphous phase transition in AlN is structurally reversible but pressure leads to a permanent densification by probably removing free volumes.

The HDA phase of semiconducting materials frequently presents metallic character. Since some high-tech applications of *a*-AlN depend on its electronic properties, we finally explore the influence of pressure on electronic structure of *a*-AlN using total and partial electron density of states (EDOS and PDOS). Figure 8 shows the computed EDOS near band gap region for selected pressures. At ambient condition, the band gap energy is about 1.7 eV and it has a trend to increase nonlinearly with the application of pressure. One

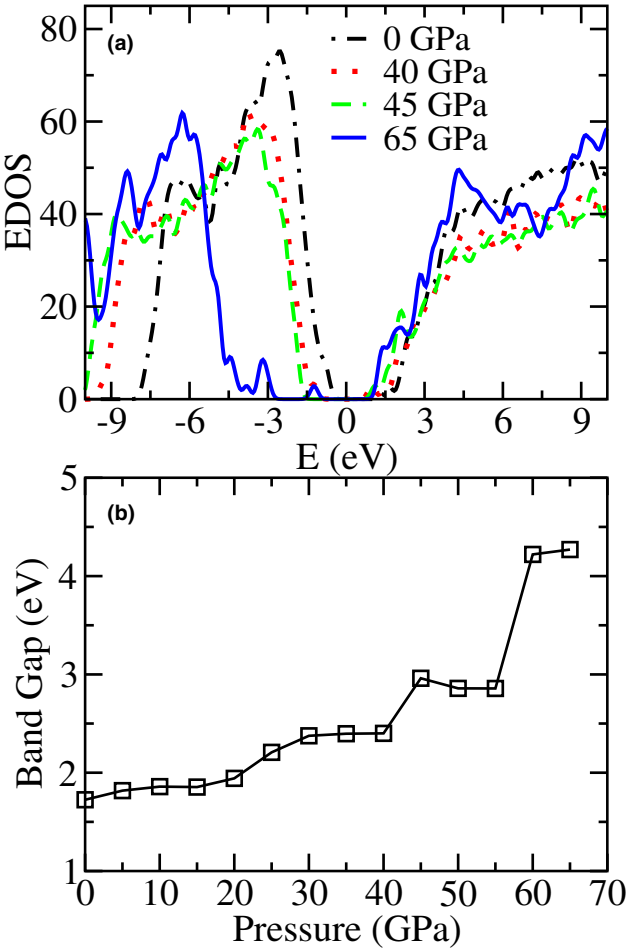

Fig. 8. (a) Electron density of state (EDOS) near band bap energy at selected pressures (b) Variation of band gap energy under pressure.

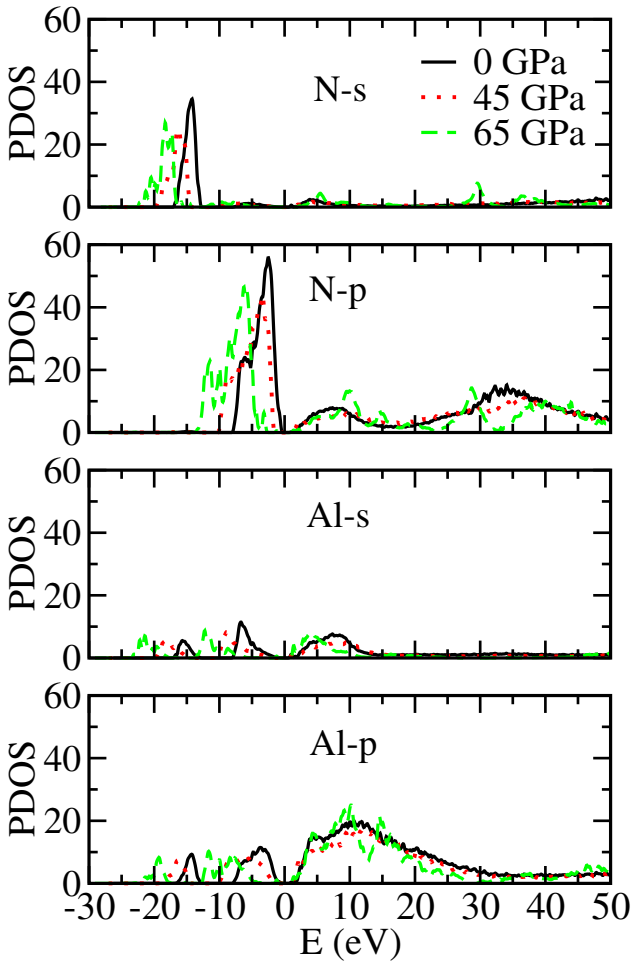

Fig. 9. Partial density of states at selected pressures.

can see that both valence and conduction states shift to lower energies with increasing pressure but the shift of the valence states is more than that of conduction states, resulting into an increase in the band gap energy. Indeed, the gap width of the WZ phase was also found to be very sensitive to pressure and increased gradually with increasing pressure[39] and the RS crystal had a wider gap than WZ state (using the same simulation technique, the band gap of the WZ and RS phases at zero pressure was calculated to be about 3.75 and 4.12 eV, respectively). So one can see that *a*-AlN exhibits a parallel behavior with the WZ phase. The midgap states around −1.2 eV at 65 GPa are attributed to the structural defects because the perfect RS crystal does not present such states. To have more information about the electronic structure, we provide the PDOS in Fig. 9. The energy band levels near −15 eV have contributions from N-s states. The upper valance band near the Fermi Level is due to the N-p states. The lower conduction band near the Fermi level is dominated by Al-s and Al–p states. The plane-wave basis density functional theory pseudopotential method also reported similar findings for the crystalline phases.[66] As discussed above, pressure significantly influences the position of the energy levels (bands) but has minor effect on the contribution of these orbitals to PDOS, another word; no significant charge transfer is observed between orbitals with application of pressure. The most important conclusion of the electronic structure calculations is that a pressure-induced metallization is not likely in *a*-AlN.

IV. Discussion

The thermodynamic description of amorphous-to-amorphous phase transformations is of particular interest. The transformation can be first order such that the CN drastically changes with a noticeable volume drop as observed in Si,[42,43,46] Ge,[49,50] ice[41] or it can proceed gradually without showing a sharp volume collapse as seen in other amorphous networks for example SiO_2,[48,54,58,67] GeO_2,[55,58] $GeSe_2$,[56,57,59] GaAs,[68] GeS_2,[69–71] and SiC.[44] The phase transformation of *a*-AlN at 45 GPa in this study is interpreted as a first-order phase transformation since it is accompanied by a 6% volume collapse and a visible coordination modification. However, one might argue that the phase change at this pressure is a finite size artifact. Indeed such a dispute is likely but on the basis of our comparable findings with experiments in our earlier investigations on amorphous systems having a size of around 216 atoms or less,[42,45,50,56,68,69] we can state that constant pressure *ab initio* techniques usually capture the thermodynamic nature of amorphous-to-amorphous phase transformations in spite of a small size of simulation cells. Yet the amount of volume drops and transformation pressures as discussed below might not be comparable with experimental data.

From the previous experimental and theoretical investigations, it can be evidently seen that only a few amorphous materials show a first-order phase transformation and amorphous compounds commonly exhibit a continuous phase transition from a LDA state to a HDA state. Indeed the physical origin of different thermodynamic nature of amorphous-to-amorphous phase transition is still a long-lasting debate. Although kinetic reason and chemical disorder are considered as for the dissimilar high-pressure behaviors, there might not be a universal explanation because the driving force for each material might depend on their unique properties or structure. Note that each material has different ionicity and local structural arrangements. Therefore, the

comparison of *a*-AlN with oxide and chalcogenide glasses is not compatible because of their ionicity or local structures but its comparison with tetrahedrally coordinated amorphous networks such as GaAs and SiC is more logical. Note that GaAs, SiC, and AlN crystallize in either ZB or WZ structures, and thus, they are anticipated to have almost similar short-range order in their amorphous state. So what drives the first-order phase change in *a*-AlN and but not in *a*-SiC or *a*-GaAs? When these systems are compared, two major differences can be effortlessly noticeable. Firstly *a*-AlN is chemically ordered and it even resists the formation of homopolar bonds at high pressure whereas *a*-GaAs[66] and *a*-SiC[44] compounds present chemical disorder at ambient condition and they cannot oppose to the creation of more homopolar bonds after a certain pressure. Secondly, *a*-AlN has three-dimensional hexagonal-like (drumlike) nanoclusters having edge-sharing units hidden in the amorphous matrix[24] while the others do not have such nanostructures. So on the basis of the comparison, here, we can speculate that the chemical disorder, the presence of nanostructures or the combination of these two might be a driving force for a distinct high-pressure behavior in *a*-AlN.

It should be noted that the hexagonal-like nanoclusters in *a*-AlN play some crucial roles during the phase transformations. Namely, they resist to transform a higher coordinated configuration while the other parts of the model mostly undergoes a noticeable coordination modification after the first phase transformation. Consequently, their presence prevents *a*-AlN from forming a very dense amorphous structure having an average CN close to six. As the applied pressure is increased further, the nanoclusters cannot oppose to deformation anymore and two atoms at the opposite vertices of hexagons come closer and form four-membered rings during the second phase transformation. Since these nanoclusters consist of edge-sharing units (fourfold-membered rings), the formation of a new bond between two atoms at the opposite vertices of hexagons yields sixfold coordination. This deformation mechanism is indeed quite similar to what has been observed in the WZ→ intermediate phases →RS transformation.[39] Subsequently, the crystallization of *a*-AlN is linked to the existence of hexagonal-like nanoclusters having edge-sharing units, which, we believe, act as nucleation centers and provide an easy transformation path to a RS state.

We also would like to comment on the critical pressures obtained in the MD simulation. Although the Parrinello–Rahman method is a practical approach to study materials under extreme conditions and provides remarkable information about phase transitions at the atomistic level that cannot be easily achievable in experiments, the technique has a major limitation. Namely, it always overestimates transition pressures due to the simulation conditions such as the size of the simulation box, the absence of surface effects, very fast pressurizing conditions, etc. Therefore, the phase transitions of *a*-AlN are expected to occur at lower pressures in experiments. Since the phase transition is reversible, we are not able to use the thermodynamic principle of equal Gibbs free energies ($G = H\text{-}ST$) to estimate accurate transition pressures for *a*-AlN. Due to the overestimated transition pressures, the amount of volume collapse at the phase transformations is also anticipated to be different in experiments.

Finally, we would like to notice the drastic structural changes at 60 GPa, just before the crystallization. We believe that the crystallization process of the HDA phase started at this pressure but it was not completed. This might be due to the limitations of the simulation mentioned above or the true behavior of *a*-AlN, that is, the crystallization occurs over wide pressure ranges.

V. Conclusions

Ab initio molecular dynamics simulations are carried out to study the high-pressure behavior of *a*-AlN. Two first-order phase transitions are proposed for *a*-AlN. The first one is an amorphous-to-amorphous (polyamorphic) phase transformation in which the LDA phase transforms into a HDA phase with a CN of 4.6. Pressure leads to a permanent densification but upon pressure release, a low-coordinated amorphous network similar to the original one is recovered and hence the polyamorhism is reversible in AlN. The physical origin of polyamorphic phase transition is attributed to the chemical order and the atomic structure of *a*-AlN, that is, the existence of nanoclusters. A very HDA phase having an average CN close to six or higher does not exist in AlN because further increase in pressure results into a transformation from the HDA phase to a RS crystal. The presence of hexagonal-like nanoclusters having edge-sharing units plays a crucial role for the crystallization of *a*-AlN. The band gap energy of in *a*-AlN increases with increasing pressure and hence the pressure-induced metallization does not occur in *a*-AlN. It is likely that the conclusion on the nature of phase transformations in *a*-AlN could depend upon the finite size of the model. Yet, we suspect that this possibility is remote because the small models (216 atoms or less) considered in our prior works[42,45,50,56,68,69] seem to have the characteristic of the phase transformations compared to available experiments. It is, nevertheless, worth repeating this type of study on a larger system.

Acknowledgment

This work was supported by the Scientific and Technical Research Council of Turkey (TÜBİTAK) under grant no: 114C100.

References

[1]H. Shultz and K. H. Thiemann, "Crystal Structure Refinement of AlN and GaN," *Solid State Commun.*, **23**, 815–19 (1977).
[2]I. Petrov, E. Mojab, R. C. Powell, J. E. Greene, L. Hultman, and J. E. Sundgren, "Synthesis of Metastable Epitaxial Zincblende-Structure AlN by Solid-State Reaction," *Appl. Phys. Lett.*, **60**, 2491–3 (1992).
[3]H. Chen, K. Chen, D. A. Drabold, and M. E. Kordesch, "Band gap Engineering in Amorphous AlGaN Alloys: Experiments and ab Initio Calculations," *App. Phys. Lett*, **77**, 1117–19 (2000).
[4]J. M. Khoshman and M. E. Kordesch, "Spectroscopic Ellipsometry Characterization of Amorphous Aluminum Nitride and Indium Nitride Thin Films," *Phys. Status Solidi (c)*, **2**, 2821–7 (2005).
[5]J. M. Khoshman and M. E. Kordesch, "Optical Characterization of Sputtered Amorphous Aluminum Nitride Thin Films," *J. Non-Cryst. Solids*, **351**, 3334–40 (2005).
[6]F. Hajakbari, M. M. Larijani, M. Ghoranneviss, M. Aslaninejad, and A. Hojabri, "Optical Properties of Amorphous AlN Thin Films on Glass and Silicon Substrates Grown by Single ion Beam Sputtering," *J. Appl. Phys.*, **49**, 095802–7 (2010).
[7]A. W. Weimer, et al., "Rapid Process for Manufacturing Aluminum Nitride Powder," *J. Am. Ceram. Soc.*, **77**, 3–18 (1994).
[8]A. V. Virkar, T. B. Jackson, and R. A. Cutler, "Thermodynamic and Kinetic Effects of Oxygen Removal on the Thermal Conductivity of Aluminum Nitride," *J. Am. Ceram. Soc.*, **72**, 2031–42 (1989).
[9]J. H. Edgar (Ed.), *Properties of Group-III Nitrides, EMIS Data Reviews Series*. IEE, London, 1994.
[10]K. A. Khor, K. H. Cheng, L. G. Yu, and F. Boey, "Thermal Conductivity and Dielectric Constant of Spark Plasma Sintered Aluminum Nitride," *Mater. Sci. Eng.: A*, **347**, 300–5 (2003).
[11]Michael. E. Levinshtien, S. L. Rumyantsev, and M. S. Shur, *Properties of Advances Semiconductor Materials*, John Wiley and Sons, Inc., Chichester, 2001.
[12]S. C. Jain, M. Willander, J. Narayan, and R. Van Overstraeten, "III-Nitrides: Growth, Characterization, and Properties," *J. Appl. Phys.*, **87**, 965–1006 (2000).
[13]A. Wilmański, M. M. Bućko, Z. Pędzich, and J. Szczerba, "Salt-Assisted SHS Synthesis of Aluminum Nitride Powders for Refractory Applications," *J. Mater. Sci. Chem. Eng.*, **2**, 26–31 (2014).
[14]C. M. Lin, T.-T. Yen, V. V. Felmetsger, M. A. Hopcroft, J. H. Kuypers, andA. P. Pisano, " Thermally Compensated Aluminum Nitride Lamb Wave Resonators for High Temperature Applications," *Appl. Phys. Lett.*, **97**, 083501–3 (2010).
[15]S. Yin, K. J. Tseng, and J. Zhao, "Design of AlN-Based Micro-Channel Heat Sink in Direct Bond Copper for Power Electronics Packaging," *Appl. Therm. Eng.*, **55**, 120–9 (2013).
[16]T. M. Tritt, (Ed.), *Thermal Conductivity: Theory, Properties, and Applications*. Kluwer Academic/Plenum Publishers, New York, 2004.
[17]M. Maqbool, H. H. Richardson, and M. E. Kordesch, "Electron Penetration Depth in Amorphous AlN Exploiting the Luminescence of AlN:Tm/AlN:Ho Bilayers Current," *Appl. Phys*, **9**, 417–21 (2009).

[18]V. Dimitrova, P. G. Van Patten, H. Richardson, and M. E. Kordesch, "Photo-, Cathodo-, and Electroluminescence Studies of Sputter Deposited AlN: Er Thin Films," *Appl. Surf. Sci*., **175–176**, 480–3 (2001).
[19]F. S. Liu, et al., "Journal of Visible and Infrared Emissions From c-Axis Oriented AlN:Er Films Grown by Magnetron Sputtering," *Appl. Phys*, **99**, 053515–19 (2006).
[20]M. L. Caldwell, et al., "Visible Emission From Amorphous AlN Thin-Film Phosphors With Cu, Mn, or Cr," *J. Vac. Sci. Technol., A*, **19**, 1894–7 (2001).
[21]M. Maqbool, I. Ahmad, G. Ali, and K. Maaz, "Energy Level Splitting and Luminescence Enhancement in AlN: Er by an External Magnetic Field," *Opt. Mater*., **46**, 601–4 (2015).
[22]M. Maqbool and T. R. Corn, "Optical Spectroscopy and Energy Transfer in Amorphous AlN-Doped Erbium and Ytterbium Ions for Applications in Laser Cavities," *Opt. Lett*., **35**, 3117–19 (2010).
[23]K. Chen and D. A. Drabold, "First Principles Molecular Dynamics Study of Amorphous $Al_xGa_{1-x}N$ Alloys," *J. App. Phys*, **91**, 9743–51 (2002).
[24]M. Durandurdu, "Uncovering Nanoclusters in Amorphous AlN: An ab Initio Study," *J. Am. Ceram. Soc*., **98**, 1095–8 (2015).
[25]Q. Xia, H. Xia, and A. L. Ruoff, "Pressure-Induced Rocksalt Phase of Aluminum Nitride: A Metastable Structure at Ambient Condition," *J. Appl. Phys*., **73**, 8198–200 (1993).
[26]M. Ueno, A. Onodera, O. Shimomura, and K. Takemura, "X-ray Observation of the Structural Phase Transition of Aluminum Nitride Under High Pressure," *Phys. Rev. B*, **45**, 10123–6 (1992).
[27]S. Uehara, T. Masamoto, A. Onodera, M. Ueno, O. Shimomura, and K. Takemura, "Equation of State of the Rocksalt Phase of III–V Nitrides to 72 GPa or Higher," *J. Phys. Chem. Solids*, **58**, 2093–9 (1997).
[28]M. R. Schwarz, et al., "Formation and Properties of Rocksalt-Type AlN and Implications for High Pressure Phase Relations in the System Si–Al–O–N," *High Pres. Res*., **34**, 22–38 (2014).
[29]N. E. Christensen and I. Gorczyca, "Calculated Structural Phase Transitions of Aluminum Nitride Under Pressure," *Phys. Rev. B*, **47**, 4307–14 (1993).
[30]J. Serrano, A. Rubio, E. Hernandez, A. Munoz, and A. Mujica, "Theoretical Study of the Relative Stability of Structural Phases in Group-III Nitrides at High Pressures," *Phys. Rev. B*, **62**, 16612–23 (2000).
[31]P. Feng, D. Chen, H. Fu, and X. Cheng, "The Phase Transition and the Elastic and Thermodynamic Properties of AlN: First Principles," *Physica B: Cond. Matter*, **403**, 4259–63 (2008).
[32]P. E. Van Camp, V. E. Van Doren, and J. T. Devreese, "High-Pressure Properties of Wurtzite-and Rocksalt-Type Aluminum Nitride," *Phys. Rev. B*, **44**, 9056–9 (1991).
[33]A. M. Saitta and F. Decremps, "Unifying Description of the Wurtzite-to-Rocksalt Phase Transition in Wide-gap Semiconductors: The Effect of d Electrons on the Elastic Constants," *Phys. Rev. B*, **70**, 035214–18 (2004).
[34]S. Saib, N. Bouarissa, P. Rodríguez-Hernández, and A. Munoz, "Structural and Dielectric Properties of AlN Under Pressure," *Physica B: Cond. Matter*, **403**, 4059–62 (2008).
[35]C. C. Silva, H. W. Leite Alves, L. M. R. Scolfaro, and J. R. Leite, "Pressure-Induced Phase Transitions and Polytypic Structures in III-Nitrides," *Phys. Stat. Sol. C*, **2**, 2468–71 (2005).
[36]I. Gorczyca, N. E. Christensen, P. Perlin, I. Grzegory, J. Jun, and M. Bockowski, "High Pressure Phase Transition in Aluminum Nitride," *Solid State. Comm*, **79**, 1033–4 (1991).
[37]Y. L. Wang, C. H. Ling, Y. Bai-Ru, and C. X. Rong, "First-Principle Calculations of Elastic Properties of Wurtzite-Type Aluminum Nitride Under Pressure," *Commun. Theor. Phys*., **49**, 489–94 (2008).
[38]J. Cai and N. Chen, "Microscopic Mechanism of the Wurtzite-to-Rocksalt Phase Transition of the Group-III Nitrides From First Principles," *Phys. Rev. B*, **75**, 134109–20 (2007).
[39]M. Durandurdu, "Pressure-Induced Phase Transition in AlN: An ab Initio Molecular Dynamics Study," *J. Alloys Comp*, **480**, 917–21 (2009).
[40]P. H. Poole, T. Grande, F. Sciortino, H. E. Stanley, and C. A. Angle, "Amorphous Polymorphism," *Comput. Mater. Sci*., **4**, 373–82 (1995).
[41]O. Mishima, L. D. Calvert, and W. Whalley, "An Apparently First-Order Transition Between two Amorphous Phases of ice Induced by Pressure," *Nature (London)*, **314**, 76–8 (1985).
[42]M. Durandurdu and D. A. Drabold, "Ab Initio Simulation of First-Order Amorphous-to-Amorphous Phase Transition of Silicon," *Phys. Rev. B*, **64**, 014101–012107 (2001).
[43]P. F. McMillan, M. Wilson, D. Daisenberger, and D. Machon, "A Density-Driven Phase Transition Between Semiconducting and Metallic Polyamorphs of Silicon," *Nat. Mater*., **4**, 680–4 (2005).
[44]V. I. Ivashchenko, P. E. A. Turchi, V. I. Shevchenko, L. A. Ivashchenko, and O. A. Shramko, "Simulations of Pressure-Induced Phase Transitions in Amorphous Si_xC_{1-x} Alloys," *Phys. Rev. B*, **71**, 165209–17 (2005).
[45]M. Durandurdu, "Ab Initio Simulation of Polyamorphic Phase Transition in Hydrogenated Silicon," *Phys. Rev B*, **73**, 035209–13 (2005).
[46]P. F. McMillan, "Polyamorphic Transformations in Liquids and Glasses," *J. Matter. Chem*, **14**, 1506–12 (2004).
[47]S. K. Deb, M. Wilding, M. Somayazulu, and P. F. McMillan, "Pressure-Induced Amorphization and an Amorphous–Amorphous Transition in Densified Porous Silicon," *Nature (London)*, **414**, 528–30 (2001).
[48]M. C. Wilding, M. Wilson, and P. F. McMillan, "Structural Studies and Polymorphism in Amorphous Solids and Liquids at High Pressure," *Chem. Soc. Rev*., **35**, 964–86 (2006).
[49]E. Principi, et al., "Pressure Induced Phase Transitions in Amorphous Ge," *Phys. Scr*., **T115**, 381–3 (2005).
[50]M. Durandurdu and D. A. Drabold, "First-Order Pressure-Induced Polyamorphism in Germanium," *Phys. Rev. B, Rapid Com*, **66**, 041201–4 (2002).
[51]D. Machon, F. Meersman, M. C. Wilding, M. Wilson, and P. F. McMillan, "Pressure-Induced Amorphization and Polyamorphism: Inorganic and Biochemical Systems.," *Prog. Mater Sci*., **61**, 216–82 (2014).
[52]S. M. Antao, et al., "Network Rigidity in $GeSe_2$ Glass at High Pressure," *Phys. Rev. Lett*., **100**, 115501–4 (2008).
[53]D. J. Lacks, "Localized Mechanical Instabilities and Structural Transformations in Silica Glass Under High Pressure," *Phys. Rev. Lett*., **80**, 5385–8 (1998).
[54]L. Huang and J. Kieffer, "Amorphous-Amorphous Transitions in Silica Glass, I. Reversible Transitions and Thermo-Mechanical Anomalies," *Phys. Rev. B*, **69**, 224203–13 (2004).
[55]G. Shen, et al., "Distinct Thermal Behavior of GeO2 Glass in Tetrahedral, Intermediate, and Octahedral Forms," *PNAS*, **104**, 14576–9 (2007).
[56]M. Durandurdu and D. A. Drabold, "Simulation of Pressure-Induced Polyamorphism in a Chalcogenide Glass $GeSe_2$," *Phys. Rev. B*, **65**, 104208–15 (2002).
[57]Q. Mei, et al., "Topological Changes in Glassy $GeSe_2$ at Pressures up to 9.3 GPa Determined by High-Energy x-ray and Neutron Diffraction Measurements," *Phys. Rev. B*, **74**, 14203–12 (2006).
[58]O. B. Tsiok, V. V. Brazhkin, A. G. Lyapin, and L. G. Khvostantsev, "Logarithmic Kinetics of the Amorphous-Amorphous Transformations in SiO_2 and GeO_2 Glasses Under High Pressure," *Phys. Rev. Lett*., **80**, 999–1003 (1998).
[59]L. Properzi, A. Di Cicco, L. Nataf, F. Baudelet, and T. Irifune, "Short-Range Order of Compressed Amorphous $GeSe_2$," *Sci. Rep*., **5** (2015).
[60]P. Ordejón, E. Artacho, and J. M. Soler, "Self-consistent order-N density-functional calculations for very large systems," *Phys. Rev. B*, **53**, 10441–4 (1996).
[61]N. Troullier and J. M. Martins, "Efficient Pseudopotentials for Plane-Wave Calculations," *Phys. Rev. B*, **43**, 1993–2006 (1991).
[62]A. D. Becke, "Density-Functional Exchange Energy Approximation With Correct Asymptotic Behavior," *Phys. Rev. A*, **38**, 3098–100 (1988).
[63]C. Lee, W. Yang, and R. G. Parr, "Development of the Colle-Salvetti Correlation-Energy Formula Into a Functional of the Electron Density," *Phys. Rev. B*, **37**, 785–9 (1998).
[64]M. Parrinello and A. Rahman, "Polymorphic Transitions in Single Crystals: A new Molecular Dynamics Method," *J. Appl. Phys*., **52**, 7182–90 (1981).
[65]K. Momma and F. Izumi, "VESTA 3 for Three-Dimensional Visualization of Crystal, Volumetric and Morphology Data," *J. Appl. Crystallogr*., **44**, 1272–6 (2011).
[66]Y. C. Cheng, X. L. Wu, J. Zhu, L. L. Xu, S. H. Li, and P. K. Chu, "Optical Properties of Rocksalt and Zinc Blende AlN Phases: First-Principles Calculations," *J. Appl. Phys*., **103**, 073707–11 (2008).
[67]N. Li, R. Sakidja, S. Aryal, and W. Y. Ching, "Densification of a Continuous Random Network Model of Amorphous SiO_2 Glass.," *Phys. Chem. Chem. Phys*., **16**, 1500–14 (2014).
[68]M. Durandurdu, "Pressure-Induced Amorphous-to-Amorphous Phase Transition in GaAs.," *Phys. Rev. B*, **70**, 085204–13 (2004).
[69]M. Durandurdu, "High-Density Amorphous Phase of GeS_2 Glass Under Pressure," *Phys. Rev. B*, **79**, 205202–8 (2009).
[70]M. Vaccari, et al., "Structural Changes in Amorphous GeS2 at High Pressure," *Phys. Rev. B*, **81**, 014205–10 (2010).
[71]A. Zeidler, et al., "Establishing the Structure of GeS_2 at High Pressures and Temperatures: A Combined Approach Using x-ray and Neutron Diffraction," *J. Phys. Cond. Matter*, **21**, 474217–54 (2009). □